PHYSICAL REVIEW LETTERS

Delay-Induced Excitability

Tomasz Piwonski,[1,3] John Houlihan,[1,2] Thomas Busch,[1,2] and Guillaume Huyet[1,2]

[1]*Physics Department, National University of Ireland, University College Cork, Ireland*
[2]*Tyndall National Institute, Prospect Row, Cork, Ireland*
[3]*Institute of Electron Technology, Warszawa, Poland*

We analyze the stochastic dynamics of a bistable system under the influence of time-delayed feedback. Assuming an asymmetric potential, we show the existence of a regime in which the system dynamics displays excitability by calculating the relevant residence time distributions and power spectra. Experimentally we then observe this behavior in the polarization dynamics of a vertical cavity surface emitting laser with optoelectronic feedback. Extending these observations to two-dimensional systems with diffusive coupling, we finally show numerically that delay-induced excitability can lead to the appearance of propagating wave fronts and spirals.

Excitability, originally discovered in biology and chemistry [1], has been identified to be an important concept in a variety of fields ranging from geology to nonlinear optics. It describes any stable dynamical system that exhibits pulses when the amplitude of a perturbation exceeds a fixed threshold. Once a pulse has been created, a refractory time has to pass before another excitation is possible. In spatially extended systems, this leads to the generation of excitable fronts and spiral waves, most notably occurring on the human heart and leading to fibrillation [2]. Such spirals are also commonly observed in nonlinear chemical reactions and can be described by the FitzHugh-Nagumo model [3]. In lasers, excitability has been predicted in the presence of either optical injection [4] or saturable absorption [5] and has, for example, been experimentally observed in semiconductor lasers with optical feedback [6]. This latter experiment is very interesting, as it can be described by a delayed dynamical system with a memory time associated with the external cavity length. Such delayed dynamical systems have recently been the subject of great interest as they exhibit complex deterministic and stochastic behavior [7–9]. Understanding the behavior of time-delayed dynamical systems is a first step in improving the knowledge of memory in general, whose analysis is especially important in medicine, biology, and control theory [10].

Here we demonstrate that excitability can be observed in a simple bistable dynamical system with time-delayed feedback. Our theoretical model system consists of a particle trapped in an asymmetric, double-well potential, which is continuously exposed to noise [11] and feedback. We show that the observed dynamics is similar to the excitability model of well-known, discrete three-state models [12], but that our system also exhibits coherence resonance. Using a vertical cavity surface emitting laser (VCSEL) with optoelectronic feedback, we experimentally investigate this delay-induced excitability and determine the residence time distribution (RTD). Finally, we extend

our theoretical analysis to spatially extended systems where we show the existence of excitable spiral waves.

Our analysis is based on the following stochastic differential equation:

$$\dot{x} = -\frac{dU}{dx} + \epsilon x(t - \tau) + \eta(t), \quad (1)$$

which describes an overdamped motion in a double-well potential $U(x)$ under the influence of memory. The length of the delay interval is τ, and the feedback strength is given by ϵ. Here $\eta(t)$ describes Gaussian white noise with $\langle \eta(t) \rangle = 0$ and $\langle \eta(t)\eta(t') \rangle = 2D\delta(t - t')$. In the following, we will denote the delayed state as $x_\tau = x(t - \tau)$.

Without delay ($\epsilon = 0$), random switching occurs between the two minima of the potential, $x_{l,r}$, and the dynamics can be very well described by Kramers's theory [13]. The RTD $P_{l,r}(T)$ in each well is then given by

$$P_{l,r}(T) = \gamma_{l,r} e^{-\gamma_{l,r}T}, \quad (2)$$

where the inverse of the switching rate is the so-called Kramers's time, $T_{l,r} = 1/\gamma_{l,r}$. It describes the average time between two transitions:

$$T_{l,r} = \frac{2\pi}{\sqrt{U''(x_{l,r})U''(x_0)}} \exp[\Delta U_{l,r}/D]. \quad (3)$$

Here x_0 is the position of the local maximum between the two minima $x_{l,r}$, and $\Delta U_{l,r} = U(x_0) - U(x_{l,r})$ is the potential barrier for each well.

The statistical properties of Eq. (1) for $\epsilon \neq 0$ have been analyzed recently in the case of the generic symmetric potential $U(x) = -x^2/2 + x^4/4$. Noting that the potential can be rewritten to include the delay term, $V(x) = U(x) + \epsilon x x_\tau$, it can immediately be seen that the potential barrier, and therefore the escape rates, becomes dependent on the state at the earlier time $t - \tau$ [14]. Hence, the continuous system of Eq. (1) can be approximated by a discrete two-state model, $r(t) = \pm 1$, with transition rates that depend on

the delayed state [9]. These rates depend on the relative value of $r(t)$ and $r(t - \tau)$ and are defined as p_1 if $r(t) = r(t - \tau)$ and as p_2 if $r(t) \neq r(t - \tau)$ for a symmetric potential. Tsimring and Pikovsky have recently derived the power spectrum for this model and shown the existence of coherence resonance [9]. Other works have calculated and measured the RTD [14–16].

In an excitable system, a perturbation above a certain threshold transfers an otherwise stable steady state (the resting state) into an excited state (the firing state). The system then goes through a well defined refractory cycle before returning to its initial state. During the refractory cycle it is impervious to any external perturbation and cannot "fire" a second time. It is obvious that for noise driven systems such a mechanism will lead to a higher degree of order, and several such manifestations have been discovered in recent years. The most dramatic ones are coherence resonance [17] and wave fronts and patterns such as spirals in spatially extended systems [18].

For the asymmetric potential the presence of feedback leads to a dependence of the amplitude of each potential barrier on the position of the particle at the time $t - \tau$ and the dynamics has to be described by four characteristic times. The times T_l^+ and T_l^- are the mean escape times from the left well when the particle was in the left or right well at $t - \tau$, respectively, and T_r^- and T_r^+ are the mean escape times from the right well if the particle was in the left or right well at $t - \tau$, respectively [see Fig. 1(a)].

To illustrate the excitable behavior, let us consider the case of an asymmetric potential with $T_r \ll T_l$ (for $\epsilon = 0$) such that the minimum corresponding to $x < 0$ exists for any value of the feedback, x_τ, but the minimum for $x > 0$ exists only for $x_\tau < 0$ [see Fig. 1(b)]. Let us also assume that the particle has been in the left well for $t < 0$ and it is driven by noise into the right well at $t = 0$. For small noise amplitudes ($T_r^- \gg \tau$) the particle will almost certainly remain in the right well until the value of the feedback term changes at $t = \tau$. The potential minimum on the right-hand side then disappears and the particle will move toward the remaining minimum at $x < 0$. After a further time interval τ, the potential will switch to its initial bistable shape and the process can start over again. Such a cycle is characteristic of an excitable system. The initial

state is stable under small perturbations, but large perturbations can induce a jump. The firing corresponds to the transition of the particle into the right well and the refractory time consists of the two subsequent periods, of duration τ, before the initial state is established again. During the first half of the refractory interval, the particle resides in the well $x > 0$, from which transitions are unlikely and during the second interval only one minimum is present and transitions cannot occur. This is a model for type I excitability, since close to the bifurcation point the spike rate can become arbitrarily low [11].

It is well worth pointing out that, for this process to happen, only two conditions on the time scales have to be fulfilled: the length of the feedback interval has to be larger than the typical interwell relaxation times and shorter than the Kramers's time in the right well.

To show that the dynamics described can be observed from Eq. (1) we have numerically calculated the RTDs in the excitable regime. The potential was chosen to be

$$U(x) = -\frac{1}{2}x^2 + \frac{1}{4}x^4 + \frac{1}{3}\kappa x^3, \qquad (4)$$

with $\kappa = 0.3$, and the feedback strength was adjusted to $\epsilon = 1/3$. Assuming that the particle has made a transition into the right well (the system has fired) at the time $t = 0$, one can clearly see from Fig. 2 that the transition probability back into the left well (dashed line) is effectively zero in the interval $[0, \tau]$. The spike appearing for $T > \tau$ then indicates the potential-driven rollover to the left well and a further interval of length τ starts, in which no transitions are possible (solid line). After the sign of the feedback has changed again, the distribution follows Kramers's law for $t > \tau$. The existence of a refractory time that forbids firing twice in an interval of 2τ is therefore clearly visible from Fig. 2. Note that the inset of Fig. 2 shows the existence of higher order effects for the stochastic transition [16].

Our system can be seen as a continuous realization of a discrete three-state model [12,19], in which only the firing transition is stochastic. The refractory state is split into two states, and the transition between these two states as well as the transition back into the resting state are deterministic
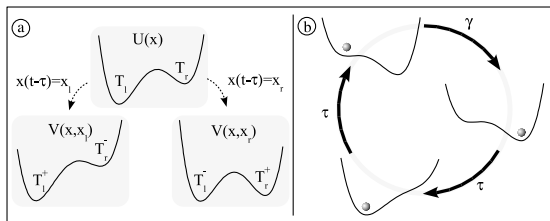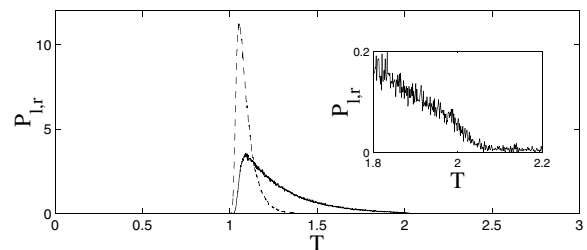
FIG. 1.   (a) Schematic definition of Kramers's residence times for an asymmetric potential without (upper graph) and with (lower graphs) negative feedback. (b) Schematic of the potentials during one excitable cycle.

FIG. 2.   Numerical RTDs for the left (solid line) and right wells (dashed line). The x axis is scaled in units of the delay interval ($\tau = 1$). The inset shows the change in slope at $T = 2$ for particles in the left well, which is due to a higher order effect in the feedback strength [16].

with fixed waiting times. It has been shown that for the discrete model the power spectrum can be calculated analytically [20]:

$$S(\omega) = \frac{2 - 2\cos(\omega\tau)}{(\gamma + 2\gamma^2\tau)[1 - \cos(2\omega\tau) + \frac{\omega}{\gamma}\sin(2\omega\tau) + \frac{\omega^2}{2\gamma^2}]},$$

(5)

and we show in Fig. 3 a comparison with the power spectrum calculated numerically from solutions of the Langevin Eqs. (1) with the potential of Eq. (4). Both curves are qualitatively similar and show their maxima close to odd multiples of π and minima at even multiples of π. However, it must be noted that, while for the discrete model the coherence is an increasing function with noise [12,19], for the continuous model it is maximized for a finite noise strength, due to the inherent stochastic nature of all transitions involved.

Excitability has been observed in the intensity of semiconductor lasers with optical feedback [21]. Here we experimentally analyze the polarization dynamics of a VCSEL with optoelectronic feedback as described in [14,16]. The light emitted by a VCSEL is usually linearly polarized, but, as the injection current increases, the emission axis will switch between the two orthogonal states. Around this switching point, one can find a current range in which the light polarization randomly switches between the two axes. Previous experiments have been designed using these lasers to study Kramers's law [22], stochastic resonance [23], and the properties of noisy time delay dynamical systems [14,16]. It is worthwhile noticing that the shape of the potential changes with the bias current applied to the laser. At the center of the bistable region both polarizations occur with the same probability and the associated potential is symmetric, while it becomes asymmetric as the injection current is varied toward the bound-
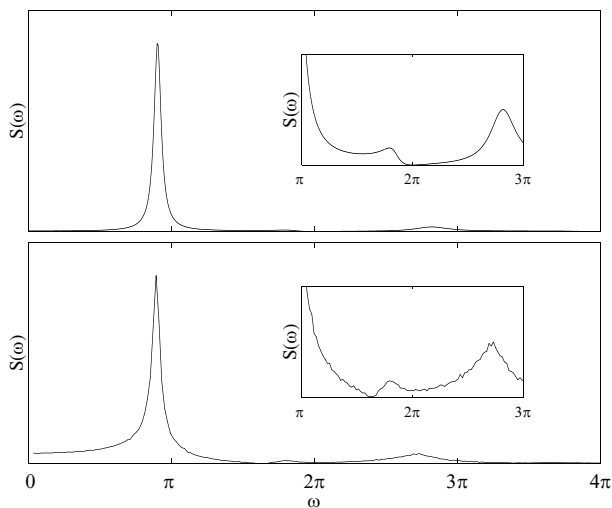
ary of the bistable region. To observe delay-induced excitability, our laser was operated in this region.

In Fig. 4 we show the RTDs measured in the excitable regime, using only the intrinsic noise of the system, where P_x, P_y refer to the two orthogonal, linear polarization states. The absence of switching events for times less than τ is clearly visible, and both the stochastic nature of the firing transition and deterministic nature of the refractory cycle can be seen from the spread of switching times being much less for P_y than P_x. When noise was introduced externally, we were also able to confirm the appearance of coherence resonance through an increase in the coherence time by about 5% as the rms voltage increased, followed by a decrease for higher voltages. At the resonance point, the combined noise in the system is due to the external noise generator added to the internal spontaneous emission noise. Unfortunately, quantifying these noise levels is a difficult task, due to the complicated nature of the spontaneous emission noise and the lack of knowledge of the noise-free characteristics of the equivalent bistable potential. Thus quantitative comparison with the previous simulations is not feasible; however, the occurrence of coherence resonance experimentally is a further indicator of the excitable nature of the system.

Let us extend the above results to arrays of stochastic units with diffusive coupling, for which it is known that the ability to sustain spatiotemporal ordering such as wave propagation and spiral patterns is a characteristic property of excitable systems [18,24]. The modified Langevin equation for this situation can be written as

$$\frac{\partial s}{\partial t} = s - \kappa s^2 - s^3 - \epsilon s_\tau + \sqrt{2D}\xi + \nabla^2 s. \quad (6)$$

Let us choose each element of the system to be initially in the resting state. At some point the noise will trigger one of the elements to fire and the coupling to neighboring elements will lead to short time correlations: to reduce the "kinetic energy" between two neighboring elements, they will also undergo a transition into the firing state. After the refractory time the elements will transfer back into the initial state, marking the end of the wave front. However, due to higher order effects in the feedback strength [16],
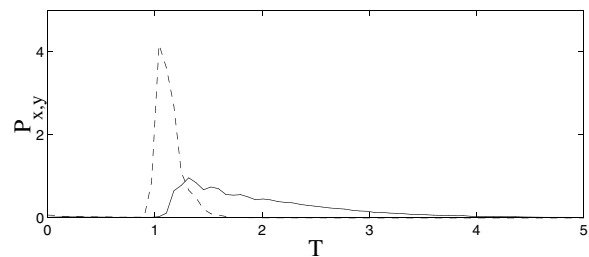

FIG. 3. Power spectrum of the discrete (upper panel) and the continuous model (lower panel). Here $\tau = 1$, $\epsilon = 0.33$, $\kappa = 0.3$.

FIG. 4. Experimental RTDs for the x (solid line) and y (dashed line) polarization of the VCSEL. Excitability is clearly visible from absence of transition probabilities for times shorter than τ. The x axis is scaled in units of the delay interval ($\tau = 1$).
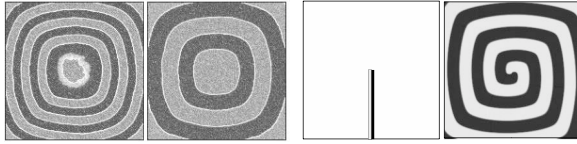
FIG. 5.   Left: Two-dimensional wave surfaces. The delay time in the left panel is twice the value of the delay time in the right panel. Right: Spiral pattern emerging from the initial condition (left panel) as described in the text. The parameters here are $\tau = 80$, $\epsilon = 0.343$, $\kappa = 0.07$, and $D = 0$. The boundary conditions for all simulations are periodic with a grid size of 2^8 points and a time step of $\delta t = 0.4$. Note that the figures show only a section of the whole integrated area, but that all figures are of the same size.

the states at the end of the refractory time do not have the same Kramers's time as the initial ones. In fact, for negative feedback the new Kramers's time is much smaller and these elements are more prone to being excited again, leading to the continuous creation of waves with wavelength τ. In Fig. 5 (left) we show two examples of such waves, obtained from numerical integration of Eq. (6). The delay time of the system on the right is twice as long as in the system shown on the left, and the two dominating colors represent the two refractory states at $s > 0$ and $s < 0$. These ordered waves can only be sustained at an optimal noise level, since too little noise will not lead to any excitations whereas too much noise will lead to fragmentation of the wave fronts.

Instead of using noise to trigger the spatial ordering, one can also choose appropriate initial conditions. In Fig. 5 (right) the appearance of spiral patterns is demonstrated by preparing a system with one area (black), where the elements have just fired after having been in the resting state for $[-\tau, 0[$. A neighboring area (gray) has just made the transition back into the resting state, while having been in the refractory state for $[-\tau, 0[$. The rest of the system (white) is in the resting state and has been there for $[-\tau, 0]$. Integrating from these initial conditions leads to a spiral pattern [see Fig. 5 (right)].

In summary, we have presented a new model of excitability that is based on stochastic bistable systems with delay. We have calculated the RTDs of the model and confirmed the absence of transition probabilities during the refractory cycle. We have also compared our continuous model to a discrete model and have shown a very good agreement of the power spectra. Using a VCSEL with optoelectronic feedback in the bistable regime, we have experimentally verified our findings and also reported the existence of coherence resonance. Finally, we have extended our model to diffusively coupled arrays and have demonstrated the appearance of spatiotemporal order in the form of waves and spirals.

[1] R. FitzHugh, Bull. Math. Biophys. **17**, 257 (1955); F. Brink *et al.*, Ann. N.Y. Acad. Sci. **47**, 457 (1946); A. T. Winfree, *The Geometry of Biological Time* (Springer, New York, 1980).

[2] J. M. Davidenko, A. V. Pertsov, R. Salomonsz, W. Baxter, and J. Jalife, Nature (London) **355**, 349 (1992).

[3] R. A. FitzHugh, Biophys. J. **1**, 445 (1961); J. Nagumo, S. Arimoto, and S. Yoshizawa, Proc. IRE **50**, 2061 (1962).

[4] P. Coullet, D. Daboussy, and J. R. Tredicce, Phys. Rev. E **58**, 5347 (1998).

[5] F. Plaza, M. G. Velarde, F. T. Arecchi, S. Boccaletti, M. Ciofini, and R. Meucci, Europhys. Lett. **38**, 85 (1997).

[6] M. Giudici, C. Green, G. Giacomelli, U. Nespolo, and J. R. Tredicce, Phys. Rev. E **55**, 6414 (1997).

[7] T. Ohira and J. G. Milton, Phys. Rev. E **52**, 3277 (1995); T. Ohira, Phys. Rev. E **55**, R1255 (1997); T. Ohira and T. Yamane, Phys. Rev. E **61**, 1247 (2000).

[8] S. Guillouzic, I. L'Heureux, and A. Longtin, Phys. Rev. E **59**, 3970 (1999); **61**, 4906 (2000).

[9] L. S. Tsimring and A. Pikovsky, Phys. Rev. Lett. **87**, 250602 (2001).

[10] N. B. Janson, A. G. Balanov, and E. Schöll, Phys. Rev. Lett. **93**, 010601 (2004).

[11] B. Lindner, J. García-Ojalvo, A. Neiman, and L. Schimansky-Geier, Phys. Rep. **392**, 321 (2004).

[12] T. Prager, B. Naundorf, and L. Schimansky-Geier, Physica (Amsterdam) **325A**, 176 (2003).

[13] H. Kramers, Physica (Utrecht) **7**, 284 (1940).

[14] J. Houlihan, D. Goulding, Th. Busch, C. Masoller, and G. Huyet, Phys. Rev. Lett. **92**, 050601 (2004).

[15] C. Masoller, Phys. Rev. Lett. **90**, 020601 (2003).

[16] D. Curtin, S. P. Hegarty, D. Goulding, J. Houlihan, Th. Busch, C. Masoller, and G. Huyet, Phys. Rev. E **70**, 031103 (2004).

[17] A. S. Pikovsky and J. Kurths, Phys. Rev. Lett. **78**, 775 (1997).

[18] J. García-Ojalvo, J. M. Sancho, *Noise in Spatially Extended Systems* (Springer, New York, 1999).

[19] A. Ñikitin, Z. Néda, and T. Vicsek, Phys. Rev. Lett. **87**, 024101 (2001).

[20] R. L. Stratonovich, *Topics in the Theory of Random Noise* (Gordon and Breach, New York, 1963).

[21] M. Giudici, C. Green, G. Giacomelli, U. Nespolo, and J. R. Tredicce, Phys. Rev. E **55**, 6414 (1997).

[22] M. B. Willemsen, M. U. F. Khalid, M. P. van Exter, and J. P. Woerdman, Phys. Rev. Lett. **82**, 4815 (1999).

[23] G. Giacomelli and F. Marin, Quantum Semiclass. Opt. **10**, 469 (1998).S. Barbay, G. Giacomelli, and F. Marin, Phys. Rev. E **61**, 157 (2000).

[24] A. T. Winfree, Science **175**, 634 (1972).